Journal of Ginseng Research 46 (2022) 396–407

Contents lists available at ScienceDirect

Journal of Ginseng Research

journal homepage: https://www.sciencedirect.com/journal/journal-of-ginseng-research

Research Article

20 (S)-ginsenoside Rh2 inhibits colorectal cancer cell growth by suppressing the Axl signaling pathway in vitro and in vivo

Haibo Zhang [a, 1], Jun-Koo Yi [b, 1], Hai Huang [a], Sijun Park [c], Wookbong Kwon [d], Eungyung Kim [a], Soyoung Jang [c], Si-Yong Kim [c], Seong-kyoon Choi [d, e], Duhak Yoon [a], Sung-Hyun Kim [f], Kangdong Liu [g], Zigang Dong [g], Zae Young Ryoo [c, **], Myoung Ok Kim [a, *]

[a] Department of Animal Science and Biotechnology, ITRD, Kyungpook National University, Sangju, Republic of Korea
[b] Gyeongbuk Livestock Research Institute, Yeongju, Republic of Korea
[c] School of Life Sciences, BK21 FOUR KNU Creative BioResearch, Kyungpook National University, Daegu, Republic of Korea
[d] Division of Biotechnology, DGIST, Daegu, Republic of Korea
[e] Core Protein Resources Center, DGIST, Daegu, Republic of Korea
[f] Department of Bio-Medical Analysis, Korea Polytechnic College, Chungnam, Republic of Korea
[g] China-US (Henan) Hormel Cancer Institute, Zhengzhou, China

ARTICLE INFO

Article history:
Received 3 April 2021
Received in revised form
27 June 2021
Accepted 7 July 2021
Available online 12 July 2021

Keywords:
20(S)-ginsenoside Rh2
Axl
Colorectal cancer
Xenograft

ABSTRACT

Background: Colorectal cancer (CRC) has a high morbidity and mortality worldwide. 20 (S)-ginsenoside Rh2 (G-Rh2) is a natural compound extracted from *ginseng*, which exhibits anticancer effects in many cancer types. In this study, we demonstrated the effect and underlying molecular mechanism of G-Rh2 in CRC cells in vitro and in vivo.

Methods: Cell proliferation, migration, invasion, apoptosis, cell cycle, and western blot assays were performed to evaluate the effect of G-Rh2 on CRC cells. In vitro pull-down assay was used to verify the interaction between G-Rh2 and Axl. Transfection and infection experiments were used to explore the function of Axl in CRC cells. CRC xenograft models were used to further investigate the effect of Axl knockdown and G-Rh2 on tumor growth in vivo.

Results: G-Rh2 significantly inhibited proliferation, migration, and invasion, and induced apoptosis and G_0/G_1 phase cell cycle arrest in CRC cell lines. G-Rh2 directly binds to Axl and inhibits the Axl signaling pathway in CRC cells. Knockdown of Axl suppressed the growth, migration and invasion ability of CRC cells in vitro and xenograft tumor growth in vivo, whereas overexpression of Axl promoted the growth, migration, and invasion ability of CRC cells. Moreover, G-Rh2 significantly suppressed CRC xenograft tumor growth by inhibiting Axl signaling with no obvious toxicity to nude mice.

Conclusion: Our results indicate that G-Rh2 exerts anticancer activity in vitro and in vivo by suppressing the Axl signaling pathway. G-Rh2 is a promising candidate for CRC prevention and treatment.

1. Introduction

Colorectal cancer (CRC) was the third most common cancer diagnosed and the second leading cause of cancer-related deaths in the United States in 2020 [1]. Although significant progress has been made in multimodality therapy for CRC, the overall 5-yr survival rate remains poor [2]. Surgical resection and chemotherapy are common treatment options for patients with CRC; however, recurrence and distant metastases occurs frequently. Thus, new and more effective therapeutic targets and strategies are required.

Natural products have been used for disease treatment and prevention for thousands of years. Because of their relatively low toxicity, the anticancer activity of natural product compounds has attracted significant attention from researchers [3–5]. Ginseng is a well-known herbal medicine that exhibits various pharmacological and therapeutic activities. 20 (S)-ginsenoside Rh2 (G-Rh2) is one of

* Corresponding author. Department of Animal Science and Biotechnology, ITRD, Kyungpook National University, Sangju, Gyeongsangbukdo, 37224, Republic of Korea.
** Corresponding author.
E-mail addresses: jaewoong64@hanmail.net (Z.Y. Ryoo), ok4325@knu.ac.kr (M.O. Kim).
[1] Zhang and Yi equally contributed to this work.

https://doi.org/10.1016/j.jgr.2021.07.004

the major active components of ginseng and shows potent anticancer effects in several cancer models [6–8]. G-Rh2 has been reported to suppress cervical cancer cell proliferation by inhibiting the AKT/GSK3β signaling pathway [9] and suppresses CRC cell growth by blocking the PBK/TOPK signaling pathway [7]. Moreover, G-Rh2 was reported to be effective at reversing drug resistance in several cancer types [10,11]. However, the effects and molecular mechanisms underlying G-Rh2 in CRC have yet to be fully elucidated.

Axl (also referred to Ark, Tyro7, or Ufo) is a receptor tyrosine kinase that plays an important role in the metastatic potential and overall prognosis of many solid cancers [12–17]. Axl appears to function as an oncogene in various human malignancies, including pancreatic [18], breast [19], and lung [12,20] cancers. Axl functions through several downstream pathways including the MAPK/ERK, PI3K/AKT, and STAT3 signaling pathways depending on the cancer type [21–23]. BGB324 (R248) is a selective Axl inhibitor that has recently entered phase II clinical trials in multiple cancers [15,22]. These results indicate that Axl is an attractive therapeutic target for CRC treatment.

In this study, we found that G-Rh2 suppresses CRC cell growth by inhibiting the Axl signaling pathway in vitro and in vivo. Axl highly expressed in CRC cells and promotes the growth, migration, and invasion of CRC cells. Axl knockdown or treatment with G-Rh2 suppressed tumor growth in nude mice. Our findings indicate that G-Rh2 is a candidate for the prevention and treatment of CRC.

2. Materials and methods

2.1. Reagents

G-Rh2 (>98% purity) was obtained from Chengdu Biopurify Phytochemicals Ltd. (Chengdu, China). Primary antibodies for detecting p-Axl (Tyr702), VEGFR2, Src (32G6), p-Src (Tyr416), p-PI3K (Tyr458), p-PI3K, p-AKT (Ser473), AKT, p-ERK1/2, ERK1/2, cleaved-caspase3 (Asp175), cleaved PARP, survivin, CDK4, CDK6, cyclin D1, cyclin E1, p-p38 (Thr180/Tyr182), p38, GSK-3β, p-GSK-3β (Ser9), p53, vimentin, slug, p-mTOR (Ser 2448), mTOR, E-cadherin, N-cadherin, and Bax were obtained from Cell Signaling Technology (Beverly, MA, USA). Axl, Flt-1, and β-actin were purchased from Santa Cruz Biotechnology (Santa Cruz, CA, USA).

2.2. Cell culture

Human CRC cell lines HCT15, HCT116, and DLD1 and the human colon fibroblast cell line CCD-18Co were purchased from the American Type Culture Collection (Manassas, VA, USA). HCT15 and DLD1 cells were grown in RPMI-1640 medium. HCT116 cells were grown in McCoy's 5A medium. CCD-18Co cells were grown in MEM medium. All media contained 10% FBS (Gibco) and 1% penicillin/streptomycin. All the cells were maintained in a 37°C incubator with 5% CO_2.

2.3. Cell viability assay

The Cell Counting Kit-8 (CCK-8; Dojindo, Japan) assays were used to measure cell viability. Briefly, cells were seeded into 96-well plates (1×10^3 cells/well) and exposed to varying concentrations of G-Rh2 for 0, 24, 48, and 72 h. At the corresponding time points, CCK-8 solution (10 μL) was added to each well of the plate and incubated for an additional 1 h at 37°C. The absorbance of each well was read at 450 nm using a spectrophotometer.

2.4. Anchorage-independent cell growth assay

CRC cells (8×10^3) were suspended in complete growth medium with 0.6% agar and various concentrations of G-Rh2 in the base layer and 0.3% agar with the various G-Rh2 concentrations in the top layer in 6-well plates. The plates were cultured in a cell culture incubator for 2 weeks. The number of colonies was subsequently counted using the ImageJ software.

2.5. Cell cycle distribution and apoptosis

Cells (2×10^5) were seeded in 60-mm dishes and exposed to different concentrations of G-Rh2 for 48 h. For cell cycle analysis, G-Rh2-treated cells were harvested and subsequently fixed in 70% ethanol overnight. The cells were then stained with propidium iodide (PI, 20 μg/mL). For apoptosis analysis, G-Rh2-treated cells were harvested and stained with annexin V (BioLegend, California, USA) and PI and analyzed by FACS Verse flow cytometry (BD Science, California, USA).

2.6. In vitro pull-down assay

CRC cell lysates (500 μg) were incubated with G-Rh2-Sepharose 4B (or Sepharose 4B only for the control) beads (50 μL, 50% slurry) in a reaction buffer (50 mM Tris pH 7.5, 5 mM EDTA, 150 mM NaCl, 1 mM DTT, 0.01% NP40, and 2 μg/mL bovine serum albumin) overnight at 4°C with gentle rocking. They were then washed five times with wash buffer (50 mM Tris pH 7.5, 5 mM EDTA, 150 mM NaCl, 1 mM DTT, and 0.01% NP40). Finally, protein binding was visualized by western blotting.

2.7. Immunofluorescence staining

CRC cells (1×10^5) were seeded into Lab-Tek II Chamber Slides (Thermo Fisher) and treated with different concentrations of G-Rh2 for 24 h. Cells were then fixed in 4% formaldehyde for 15 min. Following permeabilization with 0.3% Triton X-100, the cells were incubated with blocking buffer (5% bovine serum albumin in PBS) for 1 h followed by Axl antibody (1:200) overnight at 4°C. Subsequently, the cells were incubated with Alexa fluor 488-conjugated secondary antibody (Jackson ImmunoResearch Laboratories, Inc. West Grove, PA, USA) for 2 h at room temperature. After washing, the coverslips were mounted using a fluorescent mounting medium with 4′,6-diamidino-2-phenylindole (DAPI). Representative images were captured using a fluorescence microscope (Leica).

2.8. Western blotting analysis

CRC cells (1×10^6) were seeded into 100-mm dishes and exposed to 0, 20, and 40 μM G-Rh2 at 37°C. After 48 h, cells were harvested and washed with ice-cold PBS on ice. Tumor tissues (50 mg) were crushed and ground into a powder with a liquid nitrogen-cooled mortar and pestle. Cells or tissues were lysed using PRO-PREP™ lysis buffer on ice for 40 min. The mixture was centrifuged and supernatants was collected. A total of 30 μg of protein was loaded and separated on SDS-PAGE gels (8%–12%) and transferred onto PVDF membranes (0.22 μm, Merck Millipore). The membranes were blocked using 5% BSA for 1 h and incubated with primary antibodies at 4°C overnight. The following day, the membranes were incubated with an HRP-conjugated secondary antibody for 1 h at room temperature. Signals were developed with an ECL detection kit and visualized with the Da Vinci Fluorescence Imaging System (Da Vinci-K, Seoul, Korea).

2.9. Transfection

The pcDNA Axl plasmid was a gift from Rosa Marina Melillo (Addgene plasmid #105932) [24]. The transfection experiments were carried out using FuGENE® HD transfection reagent (Promega) following the manufacturer's instructions. To establish stable Axl-overexpressing cell lines, the transfected cell lines were exposed to 600 μg/mL of G418 (Invitrogen) for 2 wk. The selected cells were used in subsequent experiments.

2.10. Lentiviral production and infection

For Axl knockdown in CRC cells, five lentiviral human Axl shRNA vectors were purchased from Sigma-Aldrich company (SHCLNDNM_021913; among them sh-Axl#2 sequence: 5′-CCGGGCGGTCTGCATGAAGGAATTTCTCGAGAAATTCCTTCATGCAGA CCGCTTTTT-3′; sh-Axl#5 sequence: 5′-CCGGGCTGTGAAGACGATGAAGATTCTCGA GAATCTTCATCGTCTTCACAGCTTTTT-3′). Next, 293T cells were cotransfected with pLKO.1-scrambled, sh-Axl#2, and sh-Axl#5 vectors and packaging plasmids (pMD2.G, pMDLg/p RRE, and pRSV-Rev) using the FuGENE® HD transfection reagent. After 48 h, the lentiviruses were harvested by filtration using a 0.45 μm filter. The cultured HCT116 cells were infected with lentiviruses using 8 μg/mL of polybrene (Sigma). After 24 h of infection, the medium was replaced with fresh complete growth medium containing 2 μg/mL of puromycin for 2 days. The selected cells were used for subsequent experiments.

2.11. In vivo xenograft model

BALB/c-nu mice (male, aged 5–6 weeks) were purchased from Orient Bio Inc. (Seongnam, Gyeonggi, Korea). All animal experiments were performed under protocols approved by and accordance with the guidelines of the Kyungpook National University Animal Use and Care Committee (2015-0135). HCT116 cells were collected in PBS at a final concentration of 1×10^7 cells/mL. The cells (200 μL) were subcutaneously injected into the flanks of mice. Twelve days after injection, the mice were randomly divided into three groups (n = 6 mice/group) and treated with an intraperitoneal injection of G-Rh2 (10 mg/kg and 50 mg/kg) or vehicle (PBS) three times a week for 21 days. For Axl knockdown xenograft assays, the mice were randomly divided into two groups (n = 4 mice/group) and sh-Mock or sh-Axl#2 HCT116 cells (5×10^6 cells in 0.2 mL PBS) were subcutaneously injected into the flanks of each mouse. Tumor volumes and body weights were recorded every 4 days. Tumor volumes were assessed using the following formula: (length × width × height × 0.52).

2.12. Immunohistochemical analysis

Tissue samples from mice were fixed with formalin and embedded in a paraffin, and cut into 4-μm sections. Next, they were hybridized with primary antibodies Ki-67 (1:500), p-AKT (1:200), p-p38 (1:800), and Bax (1:200). Finally, the sections were mounted with DPX Mountant for histological analysis.

2.13. Statistical analysis

Statistical analysis was performed using the GraphPad Prism8 software (GraphPad Software Inc. CA, USA). Statistically significant differences were tested using Student's t-test. All data represent means ± SD from at least three individual experiments. $P < 0.05$ was considered statistically significant.

3. Results

3.1. G-Rh2 suppresses CRC cell growth without toxicity to normal colon fibroblast cells

To explore the anticancer activity of G-Rh2 in CRC cells, we investigated the effect of G-Rh2 on cellular response. We treated HCT15, HCT116, and DLD1 cells with 0, 10, 20, 40, or 60 μM G-Rh2 for 24 h in 6-well plates. After 24 h of treatment, we observed that CRC cell density significantly decreased compared with control cells at 40 μM G-Rh2 and most of the cells were dead at 60 μM (Fig. S1). Next, we used a CCK-8 assay to evaluate the cell viability of HCT15, HCT116, and DLD1 cells after treatment with various concentrations of G-Rh2 for 24 h. The results showed that G-Rh2 inhibited cell viability in a concentration-dependent manner and the IC_{50} values for G-Rh2 on HCT15, HCT116, and DLD1 cells were 39.50, 40.81, and 46.16 μM, respectively (Fig. 1B). The viability of the CCD-18Co normal human colon fibroblast cell line was not affected by G-Rh2 treatment, even at 80 μM (Fig. 1B). Therefore, 0, 10, 20, and 40 μM of G-Rh2 were selected for additional in vitro studies. The CCK-8 assay results revealed that G-Rh2 significantly inhibited the proliferation of CRC cells in a dose- and time-dependent manner (Fig. 1C). Besides, G-Rh2 markedly reduced the number of colonies in an anchorage-independent cell growth assay (Fig. 1D and E). Collectively, these results indicate that G-Rh2 exhibits potent antigrowth activity in CRC cells with minimal cytotoxic effects on normal colon fibroblast cells.

3.2. G-Rh2 inhibits the migration and invasion of CRC cells

To explore the effect of G-Rh2 on the migration and invasion capacity of CRC cells, wound-healing and transwell assays were conducted. The wound-healing assay results indicated that the migration of HCT15, HCT116, and DLD1 cells was significantly inhibited following treatment with G-Rh2 for 12 and 24 h compared with the control. (Fig. 2A and B). Next, we performed transwell assays to further verify the effect of G-Rh2 on the cell migration and invasion ability. The transwell assay results indicated that G-Rh2 inhibited the migration and invasion capacity of CRC cells in a dose-dependent manner (Fig. 2C–F). Epithelial–mesenchymal transition (EMT) is known to be closely associated with cancer cell invasion and metastasis [25], and we detected the expression of EMT markers in CRC cells after G-Rh2 treatment by western blot analysis. Specifically, N-cadherin and vimentin were downregulated and E-cadherin was upregulated following treatment with G-Rh2 in HCT15, HCT116, and DLD1 cells (Fig. 2E). These results indicate that G-Rh2 plays a role in preventing CRC metastasis.

3.3. G-Rh2 induces G_0/G_1 phase arrest and apoptosis of CRC cells

To further explore the molecular mechanisms of G-Rh2 in CRC cell growth, we used a flow cytometry assay to determine cell cycle distribution and apoptosis in CRC cell lines following G-Rh2 treatment. As shown in Fig. 3A and B, compared with the control, G-Rh2 treatment significantly increased the ratio of G_0/G_1 phase cells. Then we explored how G-Rh2 regulated cell cycle-related proteins. We found that the G_0/G_1-phase cell cycle regulatory proteins, cyclin E1, cyclin D1, CDK 4, and CDK 6, were downregulated by G-Rh2 treatment in these three cell lines (Fig. 3E). In addition, the percentage of apoptotic HCT15, HCT116, and DLD1 cells significantly increased following treatment with G-Rh2 for 48 h (Fig. 3C and D). Moreover, G-Rh2 upregulated the protein levels of the proapoptotic proteins p53, cleaved caspase3, and cleaved PARP, whereas the

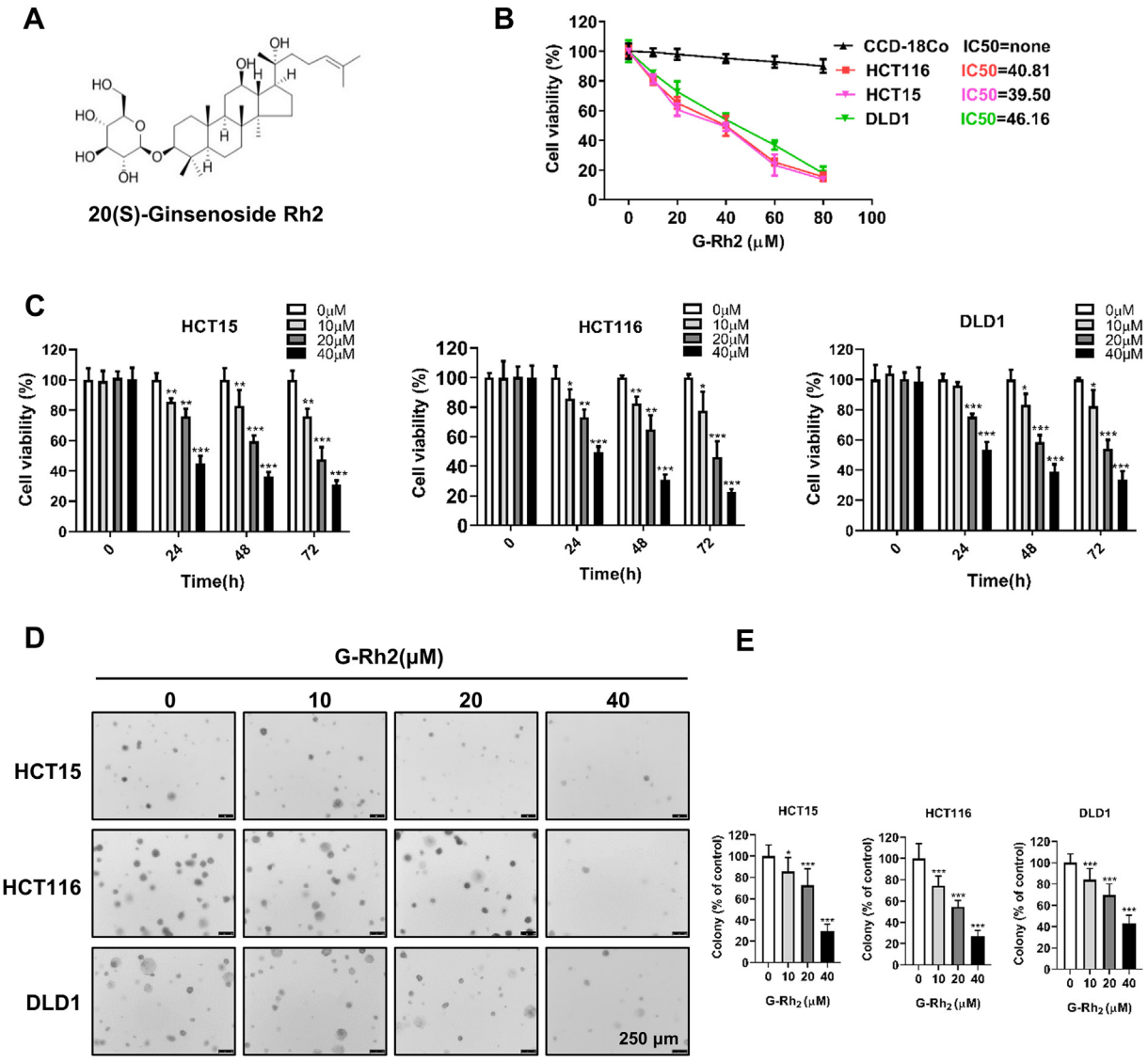

Fig. 1. G-Rh2 effectively inhibits CRC cell growth with a nontoxic effect on colon fibroblast cells. (A) The chemical structure of 20 (S)-ginsenoside Rh2. (B) HCT15, HCT116, DLD1, and CCD-18Co cells were seeded into 96-well plates and exposed to a range of concentrations of G-Rh2 for 24 h; cell viability was then determined by the CCK-8 assay. (C) HCT15, HCT116, and DLD1 cells were exposed to G-Rh2 (0, 10, 20, and 40 μM) for 0, 24, 48, and 72 h, and cell viability was determined by the CCK-8 assay. (D) and (E) Anchorage-independent growth showing colonies formed in HCT15, HCT116, and DLD1 cells after treatment with different concentrations of G-Rh2 for 12 d. Scale bar, 250 μm. $*P < 0.05$, $**P < 0.01$, $***P < 0.001$ versus control.

expression of the antiapoptotic protein survivin was down-regulated in CRC cells (Fig. 3F).

3.4. G-Rh2 directly binds to Axl and inhibits the Axl signaling pathway in CRC cells

Axl is a poor prognostic marker of colorectal cancer [26], and aberrant expression of Axl is related to cancer cell metastasis [27] and acquired drug resistance [20,28]. We found that the expression of p-Axl and Axl was higher in CRC cells (HCT15, HCT116, and DLD1) compared with CCD-18Co normal colon fibroblast cells (Fig. 4A). Some evidence indicated that G-Rh2 has a role in reversing drug resistance, such as Adriamycin-resistant breast cancer cells [29] and 5-FU resistance colorectal cancer cells [11]. Besides, G-Rh2 could regulate Axl downstream PI3K/Akt signaling pathways expression in several cancer types [30,31]. Thus, we considered whether G-Rh2 influences the Axl signaling pathway. To test this hypothesis, we performed an in vitro pull-down assay to explore whether G-Rh2 could bind with Axl proteins. The results indicated that G-Rh2 could directly bind to Axl (Fig. 4B). Besides, we found that G-Rh2 failed to bind with the receptor tyrosine kinases Flt-1 and VEGFR-2 (Fig. 4B). Then we detected the influence of G-Rh2 on Axl and its downstream protein expression by western blotting assay. We found that G-Rh2 inhibited the phosphorylation of Axl, Src, ERK, PI3K, AKT, mTOR, and GSK-3β in HCT15 and HCT116 cells (Fig. 4C). The immunofluorescence assays results showed that Axl expression was inhibited by G-Rh2 treatment in HCT15 and HCT116 cells (Fig. 4D and E). Moreover, immunoblotting results indicated that the Axl protein level was downregulated in the HCT116 membrane, but not in the cytosol (Fig. S2A). In addition, we found that G-Rh2 did not significantly decrease Axl mRNA levels (Fig. S2B). Collectively, these results indicate that G-Rh2 can directly bind to Axl and inhibit the Axl signaling pathway in CRC cells.

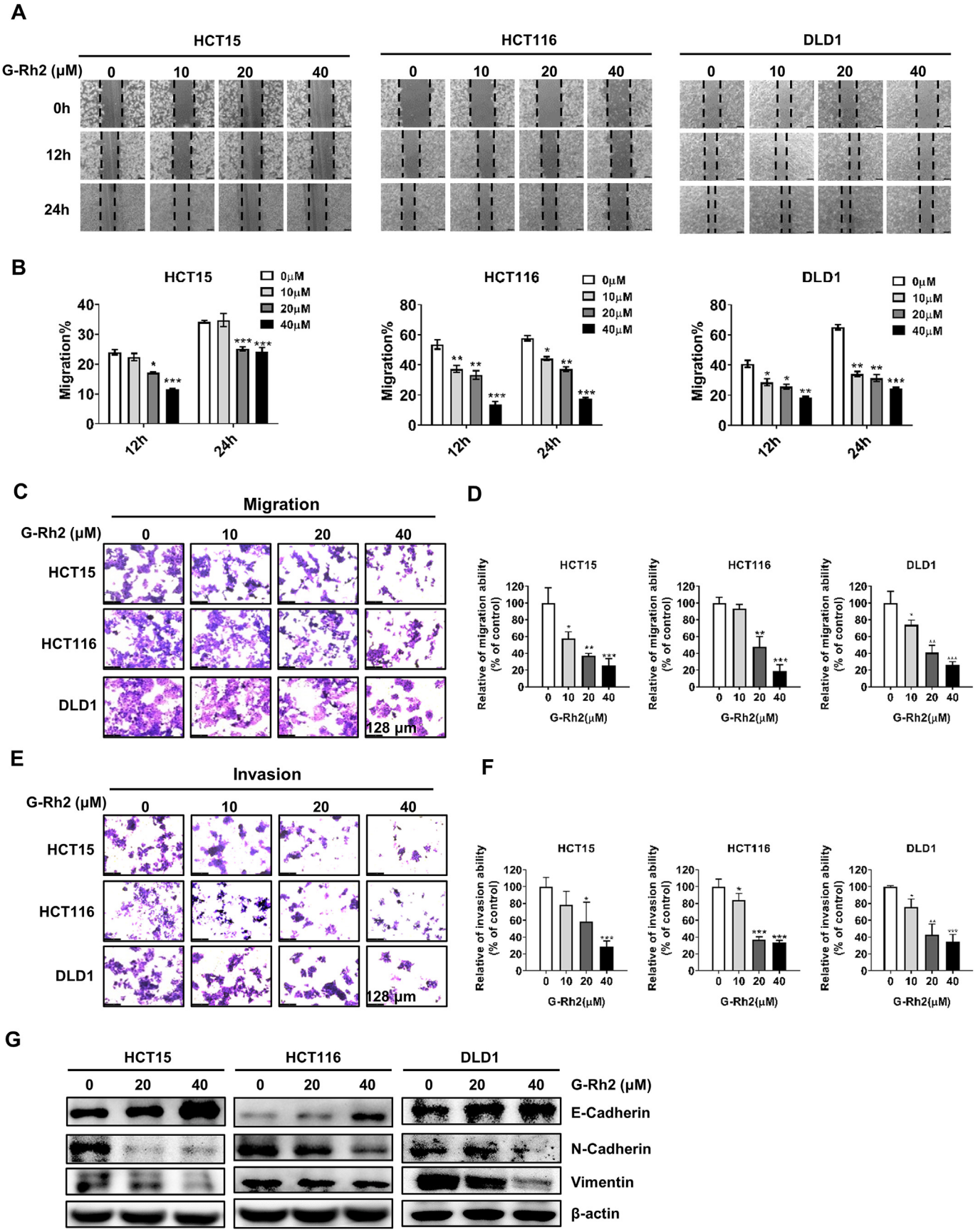

Fig. 2. G-Rh2 suppresses the migration and invasion of CRC cells. (A) and (B) Wound-healing assay in HCT15, HCT116, and DLD1 cells following treatment with G-Rh2 for 12 and 24 h, respectively (scale bar, 250 μm). (C) and (D) The migration abilities of HCT15, HCT116, and DLD1 cells were determined by transwell assay after treatment with different

3.5. Axl promotes the proliferation, migration, and invasion of CRC cells

To further investigate the functions of Axl in CRC cells, we knocked down Axl in HCT116 cells using lentiviral shRNA. Immunoblotting results showed that the Axl expression was silenced following infection with Axl shRNAs (especially sh-Axl#2 and -Axl#5) (Fig. 5A). Then, we explored the effect of Axl on CRC cell growth by various experiments. We found the cell viability was significantly inhibited in Axl knockdown cells (Fig. 5B). In addition, Axl knockdown inhibited the cell migration and invasion ability (Fig. 5C and D) and induced G_0/G_1 phase cell cycle arrest (Fig. 5E and F). Knockdown of Axl decreased the colony number in HCT116 cells, whereas G-Rh2 failed to further inhibit colony formation in Axl knockdown cells compared with the control (Fig. 5G and H), indicating that Axl was the primary target of G-Rh2 during CRC cell growth. Our in vivo study showed that Axl knockdown significantly suppressed tumor growth and decreased tumor weight in xenograft mice (Fig. 5I–K). In addition, to further verify the role of Axl in CRC cells, we established two stable Axl-overexpressing CRC cell lines (Fig. S3A). CCK-8 assays revealed that Axl overexpression significantly promoted CRC cell viability (Fig. S3B). Axl overexpression also increased the colony number in HCT15 and HCT116 cells (Figs S3C, S3D) and promoted the migration and invasion capacity of HCT15 and HCT116 cells (Figs S3E, S3F). Moreover, the overexpression of Axl diminished the effect of G-Rh2 in inhibiting the colony formation ability in HCT15 and HCT116 cells (Figs S3C, S3D). Collectively, these results indicate that Axl promotes the proliferation, migration, and invasion of CRC cells and that it is the main target of G-Rh2 to inhibit the growth of CRC cells.

3.6. G-Rh2 suppresses HCT116 xenograft tumor growth in nude mice

Based on our in vitro results, we further examined the antitumor effects of G-Rh2 in tumor-bearing mice. The xenograft model was established by subcutaneously injecting of HCT116 cells into the flanks of nude mice. After 12 days, the mice were divided into three groups, and treated with different doses of G-Rh2 for 3 weeks. The results indicated that 10 and 50 mg/kg of G-Rh2 significantly suppressed tumor growth compared with that in the vehicle-treated group (Fig. 6A and B). Meanwhile, G-Rh2 treatment reduced the protein levels of p-Axl, p-Src, p-ERK, and p-p38 in tumor tissues (Fig. 6D), which is consistent with our in vitro results. Additionally, there were no obvious differences in the histological structure of the liver and lung in these three groups, indicating that G-Rh2 was well-tolerated (Fig. 6C). Immunohistochemistry results indicated that the expression of Ki67, p-AKT, and p-p38 were significantly suppressed by G-Rh2 treatment, whereas the Bax expression was increased (Fig. 6E and F). These results indicate the HCT116 cell proliferation was inhibited and apoptosis was induced by G-Rh2 treatment in vivo. Collectively, G-Rh2 apparently inhibits HCT116 xenograft tumor growth in vivo by suppressing the Axl signaling pathway with no significant toxicity to mice. A schematic diagram for the underlying mechanism of the effects of G-Rh2 in CRC is shown in Fig. 6G.

4. Discussion

Colorectal cancer is still one of the cancers with a higher mortality rate, and it is necessary to find new treatment drugs. Accumulating evidence has indicated that many natural compounds can play a role in cancer prevention and treatment. G-Rh2 is an active component extracted from *P. ginseng* [32] that exerts potent anticancer activity in various cancers [7,33]. Previous studies indicated that G-Rh2 could inhibit CRC cell growth by activating p53 [34] and inhibiting TOPK activity [7]. In the present study, we found that G-Rh2 inhibits CRC cell growth by targeting and inhibiting the Axl signaling pathway in vitro and in vivo.

Axl has been reported to be highly expressed in several human cancers and associated with poor prognosis and drug resistance [15,35–38]. Axl is involved in cancer cell proliferation, migration, and invasion, rendering it a promising therapeutic target for cancer treatment [19,36]. Indeed, Axl has been shown to be a potential therapeutic target in $HER2^+$ breast cancer [39] and lung cancer [40]. Suppressing Axl expression effectively inhibits tumor growth in various cancer models [41–43]. In this study, we found that Axl was highly expressed in CRC cells and G-Rh2 could directly bind to Axl, resulting in the inhibition of Axl signaling pathway. Axl knockdown suppressed CRC cell growth in vitro and in vivo, indicating that Axl plays an essential role in CRC development and progression. To verify the role of Axl in the process of G-Rh2 inhibiting the growth of CRC cells, we treated Axl overexpression and Axl knockdown cells with G-Rh2. We found that Axl overexpression can attenuate the effect of G-Rh2, whereas the growth inhibition effect of G-Rh2 in Axl knockdown cells was not further enhanced. This indicates that Axl is a key target of G-Rh2, which inhibits the growth of CRC cells.

PI3K/AKT is one of the downstream pathways of Axl, which plays a considerable role in many biological processes (including cell growth [44], cell cycle regulation [45], apoptosis [46]). Axl promotes tumor metastasis and decreases chemosensitivity through the activation of the PI3K/Akt/GSK3β signaling pathway [47]. Abnormal expressions of the PI3K/AKT pathway proteins are common in cancers including CRC [48]. Several PI3K/AKT signaling pathway inhibitors have exhibited antitumor effects in cancer treatment [49–51]. In this study, G-Rh2 suppressed the p-AKT, p-mTOR, and p-GSK-3β expressions by inhibiting Axl in CRC cells. Src, which is another downstream protein of Axl [52], was reported to mediate cell growth, migration, and angiogenesis through the MAPK, PI3K, and Stat3 signaling pathways [53,54]. Src can regulate cell proliferation and cell cycle arrest by activating ERK1/2 and AKT [55,56]. In our study, G-Rh2 significantly downregulated p-Src and p-ERK1/2 expressions in CRC cells both in vitro and in vivo.

EMT is a key process that influences tumor invasion and metastasis. A direct link between EMT and metastasis has been confirmed in various tumor cell lines [57]. Upregulation of N-cadherin and downregulation of E-cadherin is the hallmark of EMT in cancer cells [58]. We found that G-Rh2 significantly inhibited CRC cell migration and invasion in vitro by reducing the expression of vimentin and N-cadherin and increasing E-cadherin in CRC cells. This demonstrates that G-Rh2 suppresses EMT in CRC cells. A role for Axl in EMT has also been reported in various cancers. For example, one study reported that Axl upregulation controls the motility of breast cancer cells driven by EMT [59]. Axl is highly expressed in advanced CRC and was significantly related to the expression of cell migration genes [16]. Our results also indicate

concentrations of G-Rh2 for 48 h (scale bar, 128 μm). (E) and (F) The invasion abilities of HCT15, HCT116, and DLD1 cells were determined using transwell assay after treatment with different concentrations of G-Rh2 for 48 h (scale bar, 128 μm). (G) Western blot analysis showing the expression of N-cadherin, vimentin, and E-cadherin in CRC cells after treatment with different concentrations of G-Rh2 for 48 h. $^*P < 0.05$, $^{**}P < 0.01$, $^{***}P < 0.001$ versus control.

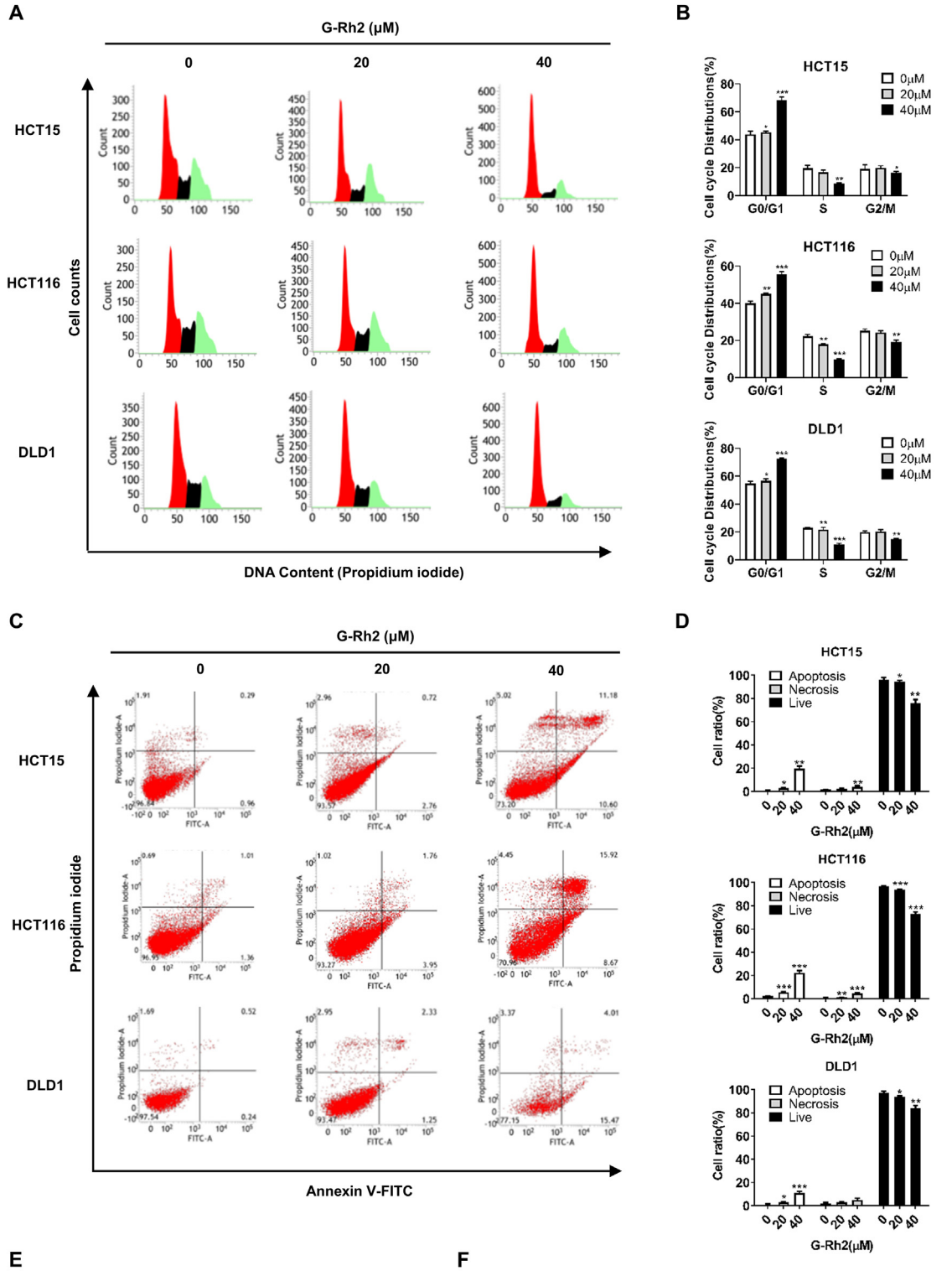
A
G-Rh2 (μM)
0
20
40
HCT15
HCT116
DLD1
Cell counts
Count
DNA Content (Propidium iodide)
B
HCT15
HCT116
DLD1
0μM
20μM
40μM
Cell cycle Distributions(%)
G0/G1
S
G2/M
C
G-Rh2 (μM)
HCT15
HCT116
DLD1
Propidium iodide
FITC-A
Annexin V-FITC
D
HCT15
HCT116
DLD1
Apoptosis
Necrosis
Live
Cell ratio(%)
G-Rh2(μM)
E
HCT15
HCT116
DLD1
G-Rh2 (μM)
Cyclin D1
CDK4
CDK6
Cyclin E1
β-actin
F
HCT15
HCT116
DLD1
G-Rh2 (μM)
P53
Cl Casp3
Cleaved PARP
Survivn
β-actin

Fig. 3. G-Rh2 induces G_0/G_1-phase cell cycle arrest and apoptosis in CRC cells. (A) and (B) Cell cycle distribution in HCT15, HCT116, and DLD1 cells treated with 0, 20, and 40 μM of G-Rh2 for 48 h were detected by flow cytometry. (C) and (D) Annexin V/PI staining (indicating apoptosis) in HCT15, HCT116, and DLD1 cells treated with 0, 20, and 40 μM of G-Rh2 for 48 h were detected by flow cytometry. (E) Expression of G_0/G_1 phase cell cycle marker proteins were detected by western blotting. (F) Expression of p53, p-p53, cleaved caspase3, cleaved PARP, and survivin in CRC cells following G-Rh2 treatment (48 h) were detected by western blotting. *$P < 0.05$, **$P < 0.01$, ***$P < 0.001$ versus control.

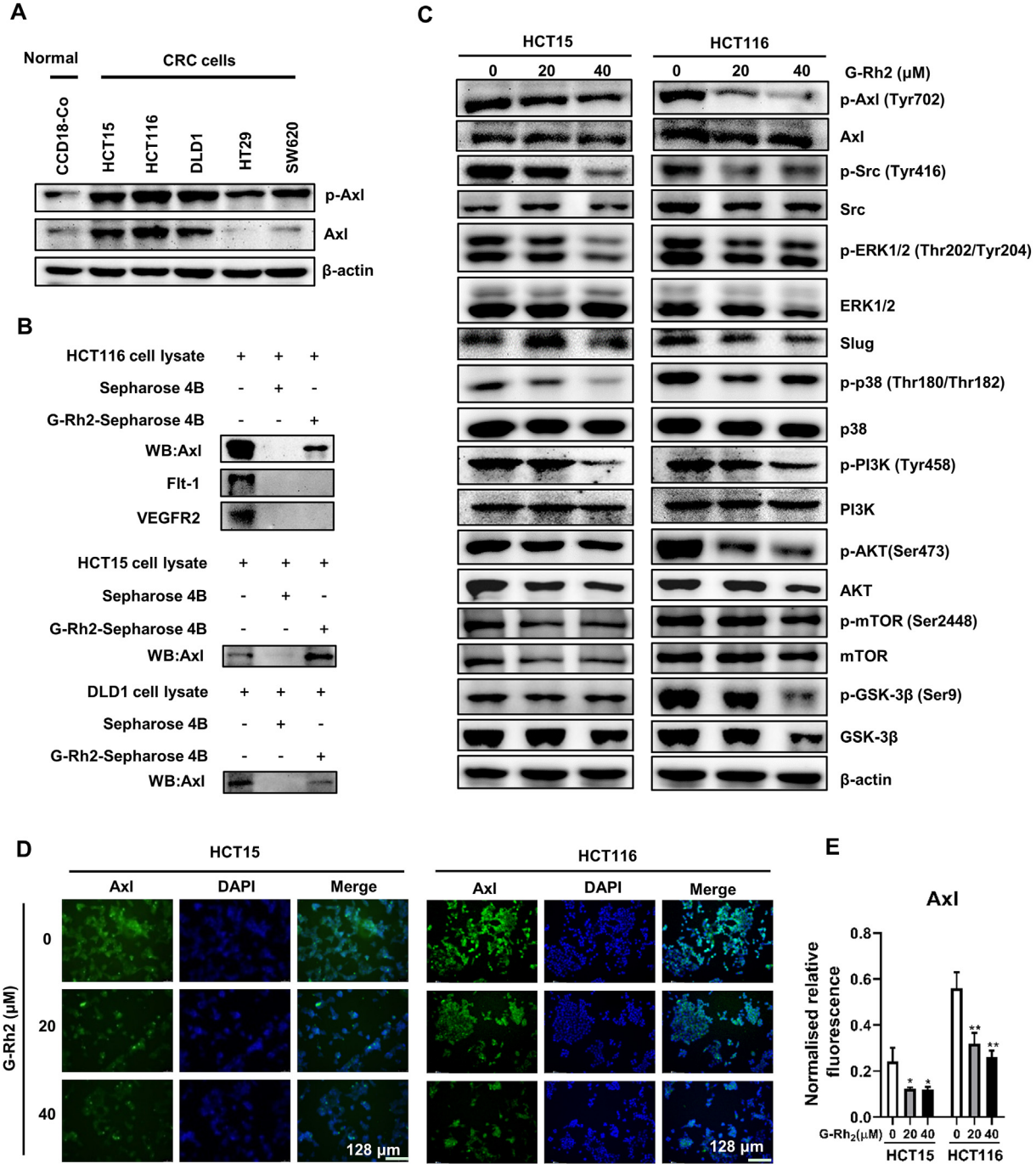

Fig. 4. G-Rh2 directly binds to Axl and inhibits the Axl signaling pathway in CRC cells. (A) p-Axl and Axl expression in CRC cells and CCD-18Co cells were detected by western blotting. (B) In vitro pull-down assays were performed, and the interaction between G-Rh2 and Axl was confirmed by western blotting. (C) The effects of G-Rh2 on Axl signaling pathway protein expression in CRC cells were determined by western blotting. (D) Immunofluorescence staining of the Axl expression in HCT15 and HCT116 cells treated with G-Rh2 for 48 h (scale bar, 128 μm). (E) Statistical results of the fluorescence intensity of Axl protein. *$P < 0.05$, **$P < 0.01$ versus control.

that Axl is involved in the EMT process and that Axl overexpression promoted the migration and invasion ability of CRC cells, whereas its knockdown resulted in the opposite effect.

Animal models are widely regarded as essential for the study of the efficacy of antitumor drugs.G-Rh2 has been reported to inhibit tumors in several cancer xenograft models including H1299 lung

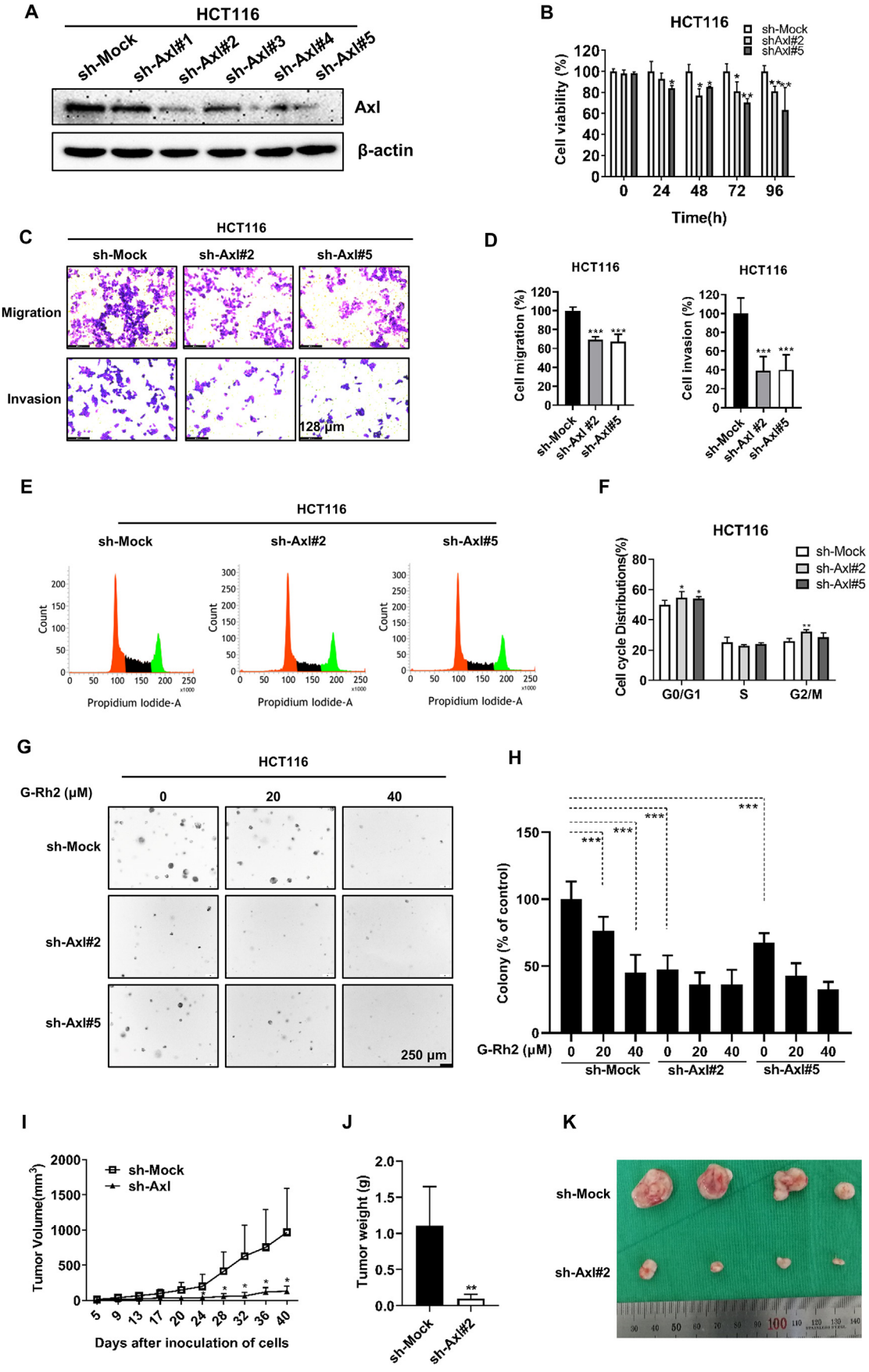

Fig. 5. Axl knockdown inhibits CRC cell growth in vitro and in vivo. (A) Axl knockdown in HCT116 cells was detected by the western blotting. (B) Cell viability in Axl knockdown HCT116 cells was determined by the CCK-8 assay. (C) and (D) Migration and invasion ability of Axl knockdown HCT116 cells (scale bar, 128 μm). (E) and (F) Flow cytometry analysis of

the cell cycle in Axl knockdown HCT116 cells. (G) and (H) Colony formation assay in Axl knockdown HCT116 cells treated with 0, 20, and 40 μM of G-Rh2 (scale bar, 250 μm). (I) Tumor volume. (J) Tumor weight. (K) Images of xenograft tumors. *$P < 0.05$, **$P < 0.01$, ***$P < 0.001$ versus control.

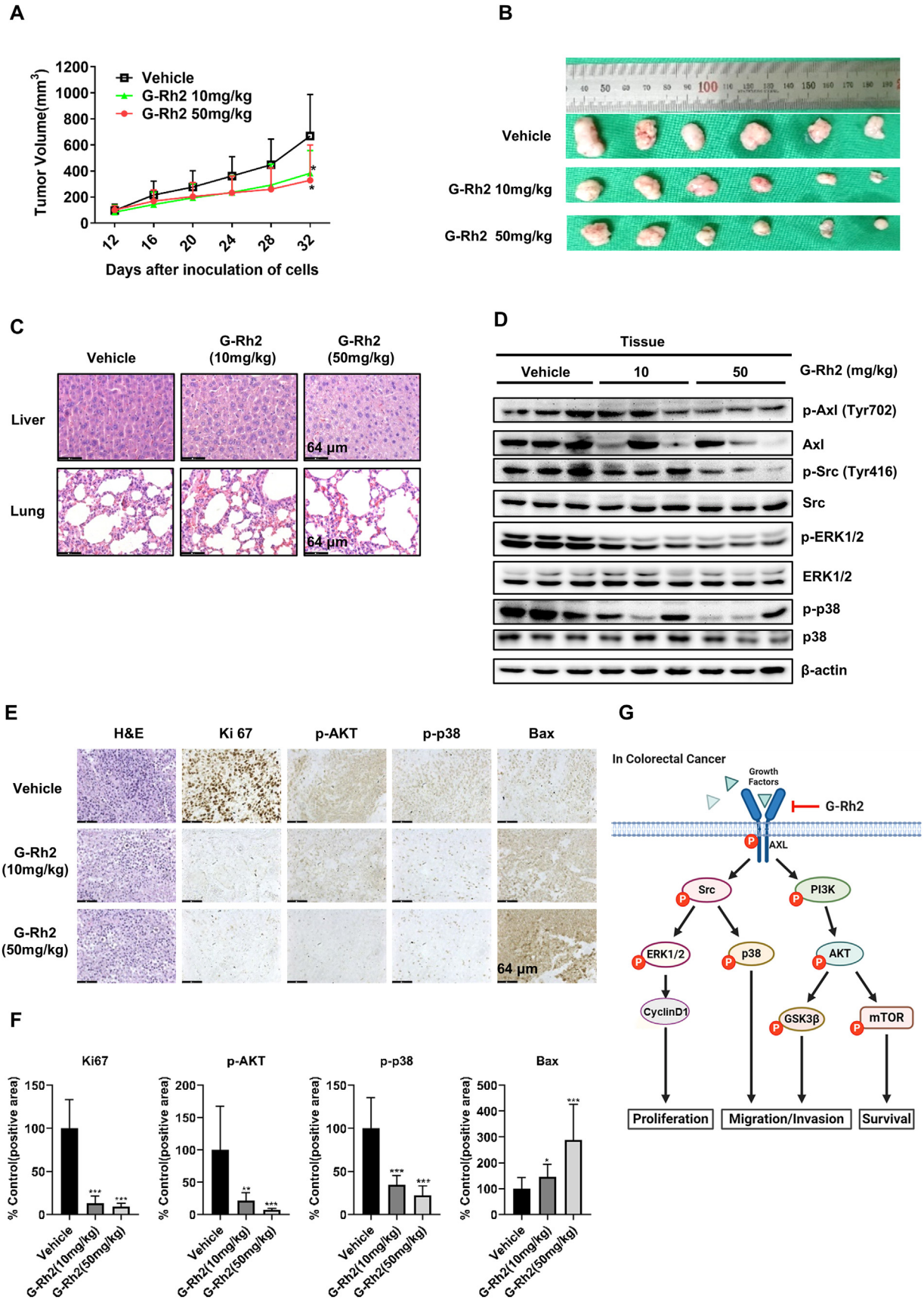

Fig. 6. G-Rh2 suppresses HCT116 cell xenograft tumor growth in nude mice. (A) Tumor growth curve was plotted according to the tumor volume and the day after treatment. Data shown are means ± SDs of tumor volume for each group (n = 6). (B) Images of tumor size in three groups excised from the mice on the 32 nd day after implantation. (C) The expression of p-Axl, Axl, p-Src, Src, p-ERK1/2, ERK1/2, p-p38, and p38 in tumor tissues was measured by western blotting. (D) H&E staining of liver and lung specimens collected from mice. (E) and (F) Immunohistochemical analysis of Ki-67, p-AKT, p-p38, and Bax in xenograft tumors tissues. (G) Schematic diagram of the underlying mechanism of the G-Rh2 effects on CRC cells. G-Rh2 binds to Axl and suppresses the Axl signaling pathway, thus inhibiting CRC cell growth, migration, and invasion. Scale bar, 64 μm. *$P < 0.05$, **$P < 0.01$, ***$P < 0.001$ versus control.

cancer cells [8] and A375 melanoma cells [60]. In this study, we investigated the antitumor effects of G-Rh2 in an HCT116-derived xenograft model and demonstrated that G-Rh2 significantly suppressed HCT116 xenograft tumor growth by inhibiting the Axl signaling pathway without obvious toxicity in nude mice.

In summary, our results indicate that G-Rh2 clearly inhibits CRC cell growth in vitro and in vivo by inhibiting the Axl signaling pathway. Our results indicate that G-Rh2 is a potential therapeutic candidate that should be further tested for use against CRC and other solid tumors.

Declaration of competing interest

The authors declare no conflict of interest.

Acknowledgements

This research was supported by Basic Science Research Program through the National Research Foundation of Korea (NRF) funded by the Ministry of Education(2020R1A4A1018280).

Appendix A. Supplementary data

Supplementary data to this article can be found online at https://doi.org/10.1016/j.jgr.2021.07.004.

References

[1] Siegel RL, Miller KD, Goding Sauer A, Fedewa SA, Butterly LF, Anderson JC, Cercek A, Smith RA, Jemal A, Sauer Goding, et al. Colorectal cancer statistics, 2020. CA Cancer J Clin 2020;70:145–64.
[2] Moghimi-Dehkordi B, Safaee A. An overview of colorectal cancer survival rates and prognosis in Asia. World J Gastrointest Oncol 2012;4:71–5.
[3] Zhao R, Choi BY, Wei L, Fredimoses M, Yin F, Fu X, Chen H, Liu K, Kundu JK, Dong Z, et al. Acetylshikonin suppressed growth of colorectal tumour tissue and cells by inhibiting the intracellular kinase, T-lymphokine-activated killer cell-originated protein kinase. Br J Pharmacol 2020;177:2303–19.
[4] Hong P, Liu QW, Xie Y, Zhang QH, Liao L, He QY, Li B, Xu WW. Echinatin suppresses esophageal cancer tumor growth and invasion through inducing AKT/mTOR-dependent autophagy and apoptosis. Cell Death Dis 2020;11:524.
[5] Li Y, Xi Z, Chen X, Cai S, Liang C, Wang Z, Li Y, Tan H, Lao Y, Xu H. Natural compound oblongifolin C confers gemcitabine resistance in pancreatic cancer by downregulating Src/MAPK/ERK pathways. Cell Death Dis 2018;9:538.
[6] Tong-Lin Wu T, Tong YC, Chen IH, Niu HS, Li Y, Cheng JT. Induction of apoptosis in prostate cancer by ginsenoside Rh2. Oncotarget 2018;9:11109–18.
[7] Yang J, Yuan D, Xing T, Su H, Zhang S, Wen J, Bai Q, Dang D. Ginsenoside Rh2 inhibiting HCT116 colon cancer cell proliferation through blocking PDZ-binding kinase/T-LAK cell-originated protein kinase. J Ginseng Res 2016;40:400–8.
[8] Ge G, Yan Y, Cai H. Ginsenoside Rh2 inhibited proliferation by inducing ROS Mediated ER stress dependent apoptosis in Lung cancer cells. Biol Pharm Bull 2017;40:2117–24.
[9] Shi X, Yang J, Wei G. Ginsenoside 20(S)-Rh2 exerts anti-cancer activity through the Akt/GSK3beta signaling pathway in human cervical cancer cells. Mol Med Rep 2018;17:4811–6.
[10] Ma J, Gao G, Lu H, Fang D, Li L, Wei G, Chen A, Yang Y, Zhang H, Huo J. Reversal effect of ginsenoside Rh2 on oxaliplatin-resistant colon cancer cells and its mechanism. Exp Ther Med 2019;18:630–6.
[11] Liu GW, Liu YH, Jiang GS, Ren WD. The reversal effect of ginsenoside Rh2 on drug resistance in human colorectal carcinoma cells and its mechanism. Hum Cell 2018;31:189–98.
[12] Kim D, Bach DH, Fan YH, Luu TT, Hong JY, Park HJ, Lee SK. AXL degradation in combination with EGFR-TKI can delay and overcome acquired resistance in human non-small cell lung cancer cells. Cell Death Dis 2019;10:361.
[13] Axelrod HD, Valkenburg KC, Amend SR, Hicks JL, Parsana P, Torga G, DeMarzo AM, Pienta KJ. AXL is a putative tumor suppressor and dormancy regulator in prostate cancer. Mol Cancer Res 2019;17:356–69.
[14] Zhang G, Wang M, Zhao H, Cui W. Function of Axl receptor tyrosine kinase in non-small cell lung cancer. Oncol Lett 2018;15:2726–34.
[15] Ludwig KF, Du W, Sorrelle NB, Wnuk-Lipinska K, Topalovski M, Toombs JE, Cruz VH, Yabuuchi S, Rajeshkumar NV, Maitra A, et al. Small-molecule inhibition of Axl targets tumor immune suppression and enhances chemotherapy in pancreatic cancer. Cancer Res 2018;78:246–55.
[16] Uribe DJ, Mandell EK, Watson A, Martinez JD, Leighton JA, Ghosh S, Rothlin CV. The receptor tyrosine kinase AXL promotes migration and invasion in colorectal cancer. PLoS One 2017;12:e0179979.
[17] Divine LM, Nguyen MR, Meller E, Desai RA, Arif B, Rankin EB, Bligard KH, Meyerson C, Hagemann IS, Massad M, et al. AXL modulates extracellular matrix protein expression and is essential for invasion and metastasis in endometrial cancer. Oncotarget 2016;7:77291–305.
[18] Song X, Akasaka H, Wang H, Abbasgholizadeh R, Shin JH, Zang F, Chen J, Logsdon CD, Maitra A, Bean AJ, et al. Hematopoietic progenitor kinase 1 down-regulates the oncogenic receptor tyrosine kinase AXL in pancreatic cancer. J Biol Chem 2020;295:2348–58.
[19] Zajac O, Leclere R, Nicolas A, Meseure D, Marchiò C, Vincent-Salomon A, Roman-Roman S, Schoumacher M, Dubois T. AXL controls directed migration of mesenchymal triple-negative breast cancer cells. Cells 2020;9:247.
[20] Okura N, Nishioka N, Yamada T, Taniguchi H, Tanimura K, Katayama Y, Yoshimura A, Watanabe S, Kikuchi T, Shiotsu S, et al. ONO-7475, a novel AXL inhibitor, suppresses the adaptive resistance to initial EGFR-TKI treatment in EGFR-mutated non-small lung cancer. Clin Cancer Res 2020;26:2244–56.
[21] Melaragno MG, Fridell YW, Berk BC. The Gas6/Axl system: a novel regulator of vascular cell function. Trends Cardiovasc Med 1999;9:250–3.
[22] Tian Y, Zhang Z, Miao L, Yang Z, Yang J, Wang Y, Qian D, Cai H, Wang Y. Anexelekto (AXL) increases resistance to EGFR-TKI and activation of AKT and ERK1/2 in non-small cell lung cancer cells. Oncol Res 2016;24:295–303.
[23] Li J, Shi C, Zhou R, Han Y, Xu S, Ma H, Zhang Z. The crosstalk between AXL and YAP promotes tumor progression through STAT3 activation in head and neck squamous cell carcinoma. Cancer Sci 2020;111:3222–35.
[24] Krishnamoorthy GP, Guida T, Alfano L, Avilla E, Santoro M, Carlomagno F, Melillo RM. Molecular mechanism of 17-allylamino-17-demethoxygeldanamycin (17-AAG)-induced AXL receptor tyrosine kinase degradation. J Biol Chem 2013;288:17481–94.
[25] Creighton CJ, Gibbons DL, Kurie JM. The role of epithelial-mesenchymal transition programming in invasion and metastasis: a clinical perspective. Cancer Manag Res 2013;5:187–95.
[26] Dunne PD, McArt DG, Blayney JK, Kalimutho M, Greer S, Wang T, Srivastava S, Ong CW, Arthur K, Loughrey M, et al. AXL is a key regulator of inherent and chemotherapy-induced invasion and predicts a poor clinical outcome in early-stage colon cancer. Clin Cancer Res 2014;20:164–75.
[27] Abu-Thuraia A, Goyette MA, Boulais J, Delliaux C, Apcher C, Schott C, Chidiac R, Bagci H, Thibault MP, Davidson D, et al. AXL confers cell migration and invasion by hijacking a PEAK1-regulated focal adhesion protein network. Nat Commun 2020;11:3586.
[28] Terry S, Abdou A, Engelsen AST, Buart S, Dessen P, Corgnac S, Collares D, Meurice G, Gausdal G, Baud V, et al. AXL targeting overcomes human lung cancer cell resistance to NK- and CTL-mediated cytotoxicity. Cancer Immunol Res 2019;7:1789–802.
[29] Zhou B, Xiao X, Xu L, Zhu L, Tan L, Tang H, Zhang Y, Xie Q, Yao S. A dynamic study on reversal of multidrug resistance by ginsenoside Rh(2) in adriamycin-resistant human breast cancer MCF-7 cells. Talanta 2012;88:345–51.
[30] Xia T, Zhang J, Zhou C, Li Y, Duan W, Zhang B, Wang M, Fang J. 20(S)-ginsenoside Rh2 displays efficacy against T-cell acute lymphoblastic leukemia through the PI3K/Akt/mTOR signal pathway. J Ginseng Res 2020;44:725–37.
[31] Li C, Gao H, Feng X, Bi C, Zhang J, Yin J. Ginsenoside Rh2 impedes proliferation and migration and induces apoptosis by regulating NF-kappaB, MAPK, and PI3K/Akt/mTOR signaling pathways in osteosarcoma cells. J Biochem Mol Toxicol 2020;34:e22597.
[32] Lü JM, Yao Q, Chen C. Ginseng compounds: an update on their molecular mechanisms and medical applications. Curr Vasc Pharmacol 2009;7:293–302.
[33] Lee H, Lee S, Jeong D, Kim SJ. Ginsenoside Rh2 epigenetically regulates cell-mediated immune pathway to inhibit proliferation of MCF-7 breast cancer cells. J Ginseng Res 2018;42:455–62.
[34] Li B, Zhao J, Wang CZ, Searle J, He TC, Yuan CS, Du W. Ginsenoside Rh2 induces apoptosis and paraptosis-like cell death in colorectal cancer cells through activation of p53. Cancer Lett 2011;301:185–92.
[35] Rankin EB, Giaccia AJ. The receptor tyrosine kinase AXL in cancer progression. Cancers (Basel) 2016;8:103.

[36] Zhu C, Wei Y, Wei X. AXL receptor tyrosine kinase as a promising anti-cancer approach: functions, molecular mechanisms and clinical applications. Mol Cancer 2019;18:153.
[37] Collina F, La Sala L, Liotti F, Prevete N, La Mantia E, Chiofalo MG, Aquino G, Arenare L, Cantile M, Liguori G, et al. AXL is a novel predictive factor and therapeutic target for radioactive iodine refractory thyroid cancer. Cancers (Basel) 2019;11:785.
[38] Cardone C, Blauensteiner B, Moreno-Viedma V, Martini G, Simeon V, Vitiello PP, Ciardiello D, Belli V, Matrone N, Troiani T, et al. AXL is a predictor of poor survival and of resistance to anti-EGFR therapy in RAS wild-type metastatic colorectal cancer. Eur J Cancer 2020;138:1–10.
[39] Goyette MA, Duhamel S, Aubert L, Pelletier A, Savage P, Thibault MP, Johnson RM, Carmeliet P, Basik M, Gaboury L, et al. The receptor tyrosine kinase AXL is required at multiple steps of the metastatic cascade during HER2-positive breast cancer progression. Cell Rep 2018;23:1476–90.
[40] Koopman LA, Terp MG, Zom GG, Janmaat ML, Jacobsen K, Gresnigt-van den Heuvel E, Brandhorst M, Forssmann U, de Bree F, Pencheva N, et al. Enapotamab vedotin, an AXL-specific antibody-drug conjugate, shows preclinical antitumor activity in non-small cell lung cancer. JCI Insight 2019;4:e128199.
[41] Bae CA, Ham IH, Oh HJ, Lee D, Woo J, Son SY, Yoon JH, Lorens JB, Brekken RA, Kim TM, et al. Inhibiting the GAS6/AXL axis suppresses tumor progression by blocking the interaction between cancer-associated fibroblasts and cancer cells in gastric carcinoma. Gastric Cancer 2020;23:824–36.
[42] Lotsberg ML, Wnuk-Lipinska K, Terry S, Tan TZ, Lu N, Trachsel-Moncho L, Røsland GV, Siraji MI, Hellesøy M, Rayford A, et al. AXL targeting abrogates autophagic flux and induces immunogenic cell death in drug-resistant cancer cells. J Thorac Oncol 2020;15:973–99.
[43] Kong L, Lu X, Chen X, Wu Y, Zhang Y, Shi H, Li J. Qigesan inhibits esophageal cancer cell invasion and migration by inhibiting Gas6/Axl-induced epithelial-mesenchymal transition. Aging (Albany NY) 2020;12:9714–25.
[44] Liu X, Song M, Wang P, Zhao R, Chen H, Zhang M, Shi Y, Liu K, Liu F, Yang R, et al. Targeted therapy of the AKT kinase inhibits esophageal squamous cell carcinoma growth in vitro and in vivo. Int J Cancer 2019;145:1007–19.
[45] Chang F, Lee JT, Navolanic PM, Steelman LS, Shelton JG, Blalock WL, Franklin RA, McCubrey JA. Involvement of PI3K/Akt pathway in cell cycle progression, apoptosis, and neoplastic transformation: a target for cancer chemotherapy. Leukemia 2003;17:590–603.
[46] Yan HZ, Wang HF, Yin Y, Zou J, Xiao F, Yi LN, He Y, He BS. GHR is involved in gastric cell growth and apoptosis via PI3K/AKT signalling. J Cell Mol Med 2021;25:2450–8.
[47] Li Y, Jia L, Ren D, Liu C, Gong Y, Wang N, Zhang X, Zhao Y. Axl mediates tumor invasion and chemosensitivity through PI3K/Akt signaling pathway and is transcriptionally regulated by slug in breast carcinoma. IUBMB Life 2014;66:507–18.
[48] Han Y, Peng Y, Fu Y, Cai C, Guo C, Liu S, Li Y, Chen Y, Shen E, Long K, et al. MLH1 deficiency induces cetuximab resistance in colon cancer via Her-2/PI3K/AKT signaling. Adv Sci 2020;7:2000112.
[49] Nunnery SE, Mayer IA. Targeting the PI3K/AKT/mTOR pathway in hormone-positive breast cancer. Drugs 2020;80:1685–97.
[50] Akbari Dilmaghani N, Safaroghli-Azar A, Pourbagheri-Sigaroodi A, Bashash D. The PI3K/Akt/mTORC signaling axis in head and neck squamous cell carcinoma: possibilities for therapeutic interventions either as single agents or in combination with conventional therapies. IUBMB Life 2021;73:618–42.
[51] Miricescu D, Totan A, Stanescu-Spinu II, Badoiu SC, Stefani C, Greabu M. PI3K/AKT/mTOR signaling pathway in breast cancer: from molecular landscape to clinical aspects. Int J Mol Sci 2020;22:173.
[52] Baumann C, Ullrich A, Torka R. Torka GAS6-expressing and self-sustaining cancer cells in 3D spheroids activate the PDK-RSK-mTOR pathway for survival and drug resistance. Mol Oncol 2017;11:1430–47.
[53] Kim HIe, Lee HS, Kim TH, Lee JS, Lee ST, Lee SJ. Growth-stimulatory activity of TIMP-2 is mediated through c-Src activation followed by activation of FAK, PI3-kinase/AKT, and ERK1/2 independent of MMP inhibition in lung adenocarcinoma cells. Oncotarget 2015;6:42905–22.
[54] Lei J, Ingbar DH. Src kinase integrates PI3K/Akt and MAPK/ERK1/2 pathways in T3-induced Na-K-ATPase activity in adult rat alveolar cells. Am J Physiol Lung Cell Mol Physiol 2011;301:L765–71.
[55] Liu H, Wu Y, Zhu S, Liang W, Wang Z, Wang Y, Lv T, Yao Y, Yuan D, Song Y. PTP1B promotes cell proliferation and metastasis through activating src and ERK1/2 in non-small cell lung cancer. Cancer Lett 2015;359:218–25.
[56] Song RX, Zhang Z, Santen RJ. Estrogen rapid action via protein complex formation involving ERalpha and Src. Trends Endocrinol Metab 2005;16:347–53.
[57] Yeung KT, Yang J. Epithelial-mesenchymal transition in tumor metastasis. Mol Oncol 2017;11:28–39.
[58] De Craene B, Berx G. Regulatory networks defining EMT during cancer initiation and progression. Nat Rev Cancer 2013;13:97–110.
[59] Vuoriluoto K, Haugen H, Kiviluoto S, Mpindi JP, Nevo J, Gjerdrum C, Tiron C, Lorens JB, Ivaska J. Vimentin regulates EMT induction by Slug and oncogenic H-Ras and migration by governing Axl expression in breast cancer. Oncogene 2011;30:1436–48.
[60] Lv DL, Chen L, Ding W, Zhang W, Wang HL, Wang S, Liu WB. Ginsenoside G-Rh2 synergizes with SMI-4a in anti-melanoma activity through autophagic cell death. Chin Med 2018;13:11.